Academic Sciences International Journal of Pharmacy and Pharmaceutical Sciences

ISSN- 0975-1491 Vol 4, Suppl 5, 2012

Research Article

# THERMODYNAMIC AND INTERFACIAL STUDIES OF PHARMACEUTICAL ACTIVE NICOTINAMIDE - VANILLIN DRUG SYSTEM

**H. SHEKHAR AND VISHNU KANT***

**Department of Chemistry, V.K.S. University, Ara-802301, India. Email: imvishnukant@gmail.com**

*Received: 31 Aug, 2012, Revised and Accepted: 09 Oct, 2012*

**ABSTRACT**

The system Nicotinamide (NA) – Vanillin (VA) has the advantage of providing a hands-on experience with conventional as well as modern methods and a serious problem solving experience during thermodynamic characterization of the present simple pharmaceutical system which is more appealing than those based upon simple metallic systems. The physical and chemical interactions between drugs can affect the chemical nature, stability, critical size and solid-liquid interface of drugs. The study covers the phase diagram, molecular interaction, thermodynamic excess and mixing functions, thermal stability, driving force of nucleation during solidification ($\Delta G_v$), critical size or radius ($r^*$) and the critical free energy of nucleation ($\Delta G^*$) at different undercoolings of binary pharmaceutical materials have been determined. Using heat of fusion data the solid-liquid interface energy ($\sigma$), grain boundary energy ($\sigma_{gb}$), the Gibbs-Thomson coefficient ($\tau$) and roughness parameter ($\alpha$) of all the alloys are evaluated by numerical method. Interface morphology of the alloys follows the Jackson's surface roughness ($\alpha$) theory and predicts the faceted growth proceeds in all the alloys of pharmaceutical materials.

**Keywords:** Phase diagram, Thermodynamic excess and mixing functions, Thermal stability, Critical radius, Interfacial energy.

## INTRODUCTION

Molecular interactions responsible for the formation of molecular complexes of active pharmaceutical ingredients[1,2] (APIs) with other compounds are important not only because of the ability to control pharmaceutical properties without changing covalent bonds but also because they can be used in the design of new materials. Much of this fundamental work was geared towards understanding the mechanisms of complex formation and determining the relative influence of intermolecular interactions in solutions (hydrogen bonds, charge-transfer forces, and other electrostatic and induction forces) that favored complex formation. In recent years, advances in supramolecular engineering and chemistry have motivated to extend research on the design of pharmaceutical materials[3] by directing molecular association of different components in the crystalline state to form binary/ternary materials of potential interest. Pharmaceutical properties of some binary materials/co-crystals have also been reported such as solubility[4], dissolution rate, hygroscopicity, and chemical stability. Binary molecular compound or solid-state complex has been used in the pharmaceutical literature since the 1950s, while the term co-crystal in binary form is found in the more recent literature.

Nicotinamide (NA) is a water soluble Vitamin $B_3$ and finds its application as a nutrient supplement in Pharmaceutical products and used in the enrichment of bread, flour, and other grain-derived products. Animal feed is routinely supplemented with nicotinamide. It is also used in multi-vitamin preparations and dietary supplement. It is used in the treatment of pellagra. It also exhibits an anti-inflammatory effect[5,6] via the inhibition of the synthesis of pro-inflammatory cytokines (tumor necrosis factor (TNF)-α, interleukin (IL)-1, IL-6,IL-8, interferon (IFN)-γ), inhibition of inducible nitric oxide synthase (iNOS), modulation of free radical scavenging, and suppression of the expression of MHC Class II and some adhesion molecules on immune cells[7]. Adverse effects seen with nicotinamide include diarrhea, dizziness, itching; nausea, stomach upset, temporary feeling of warmth and headache. It also represses antigen induced lymphocytic transformation and the inhibition of 3'-5' 58 cyclic AMP phosphodiesterase[8]. Nicotinamide may prevent Type I diabetes mellitus. It has shown the ability to block the inflammatory actions of iodides known to precipitate or exacerbate inflammatory acne[9].

Other side Vanillin (VA) is used in flavorings, fragrances, pharmaceuticals, and perfumes. It is most often used with stronger flavors and scents, such as chocolate or spices like cloves, nutmeg, or cinnamon and acts as muscle relaxant for suffering from muscles aches. It is also used as a potential agent for the treatment of Sickle Cell Anemia[10], a Blood disorder. The psychotherapeutic use of vanillin encompasses as an anti-anxiety agent[11], an anticonvulsant, and/or as a sedative (sleeping drug). It has been discovered to exhibit properties characteristic of CNS depressants in mammalian subjects. It is suitable for use in treatment of anxiety disorders, such attributes including short term muscle relaxation and impairment, suppression of small motor movements without affecting gross motor movements in the host and enhancement of the duration of barbiturate-induced loss of righting reflex. Due to devoid of nitrogen the vanillin molecule acts as a relatively safe, non-toxic tranquilizing agent. It is especially effective for short term duration after administration in these psychotherapeutic uses while being extremely safe and without causing the adverse side effects often associated with many conventional tranquilizers such as members of the benzodiazepine family. Keeping the view of better performance and efficacy of binary mixture of pharmaceutical active Nicotinamide (NA) – Vanillin (VA) system has been undertaken for the detailed thermodynamic investigations such as phase diagram, excess and mixing thermodynamic functions, activity and activity coefficient, thermal stability, interfacial energy ($\sigma$), surface roughness ($\alpha$), driving force of solidification ($\Delta G_v$) and critical radius.

## EXPERIMENTAL PROCEDURE

Nicotinamide (Thomas Baker, Bombay) and Vanillin (CS Chemicals, India) were directly taken for investigation. The melting point (experimental and literature value) of nicotinamide was found 128°C and 128-130°C while for vanillin was found 84°C and 84-86°C respectively.

The solid-liquid phase equilibrium diagram of NA-VA system were determined by the thaw-melt method[12,13]. Mixtures of different compositions were made in glass test tubes by repeated heating and followed by chilling in ice. The melting and thaw temperatures were determined in a Toshniwal melting point apparatus using a precision thermometer which could read correctly up to ± 0.1°C. The heater was regulated to give above 1°C increase in temperature in every five minutes.

Heat of fusion of materials was measured by the DTA method using NETZSCH Simultaneous Thermal Analyzer, STA 409 series unit. All the runs were carried out with heating rate 2°C/min, chart speed 10mm/min and chart sensitivity 100μv/10mv.The sample weight was 5 mg for all estimation. Using benzoic acid was a standard

substance, the heat of fusion of unknown compound was determined[14,15].

**RESULTS AND DISCUSSION**

**Phase diagram**

The phase diagram of NA-VA system determined by the thaw melt method is shown in the form of temperature-composition curve in Fig.1 and equilibrium data is reported in Table 1. The system shows the formation of a eutectic with two incongruently melting 3:2 at 99°C and 3:1 at 88°C addition compounds respectively. Such type of results was also reported previously[16]. The melting point of NA (128°C) decreases on the addition of second component VA (M.P., 84°C) and further attains minimum and then increases. Eutectic alloys E(0.82 mole fraction of VA) are obtained at 76°C. At the eutectic temperature two phases namely a liquid phase L and two solid phases ($S_1$ and $S_2$) are in equilibrium and the system is invariant. In the region indicated by L a homogenous binary liquid solution exists while the two solid phases exists below the horizontal line. In the case, in region located on the left side of the diagram a binary liquid and solid NA exist while in a similar region located on the right side of the diagram a binary liquid and the second component of the system co-exist.

$$L \underset{}{\overset{\text{Cooling}}{\rightleftharpoons}} S_1 + S_2$$

**Heat of fusion**

A eutectic alloy is recognized to not be a simple mechanical mixture of the components. But, there is considerable heat of mixing/association in the binary mixture which has been reported[17]. The values of heats of fusion of eutectic and non-eutectic alloys are calculated by the mixture law using equation

$$(\Delta H)_e = \chi_{NA}\ \Delta H_{NA} + \chi_{VA}\ \Delta H_{VA} \quad (1)$$

Where $\chi$ and $\Delta H$ are the mole fraction and the heat of fusion of the component indicated by the subscript, respectively. The value of heat of fusion of binary alloys $A_1$-$A_{12}$ and E is reported in Table 1.

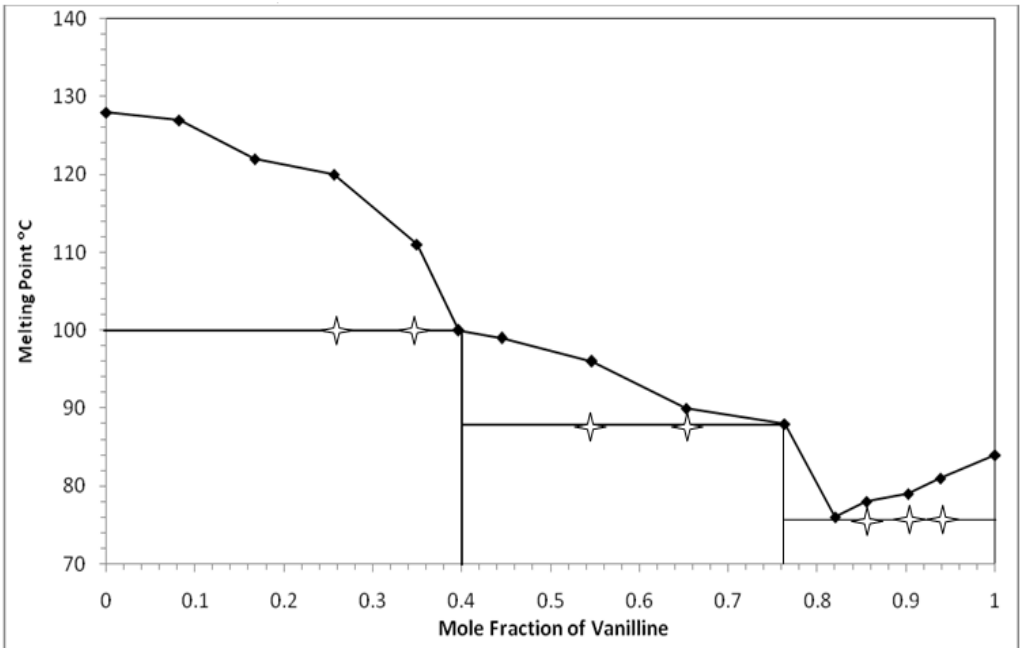


**Fig. 1: Phase Diagram of Nicotinamide-Vanilline**

■Melting Temperature Thaw melt ✧

**Table 1: Phase composition, melting temperature, values of entropy of fusion per unit volume ($\Delta S_v$), heat of fusion($\Delta H$), interfacial energy($\sigma$), grain boundary energy($\sigma_{gb}$), Gibbs-thomson coefficient ($\tau$) and roughness parameter($\alpha$)**

| Alloy | $\chi_{NA}$ | $\chi_{VA}$ | MP (°C) | $\Delta H$ (J/mol) | $\Delta S$ (J/mol/K) | $\alpha$ | $\sigma$ (kJ/m²) | $\sigma_{gb}$ (kJ/m²) | $\Delta S_v$ (J/cm³/K) | $\Delta H_v$ (J/cm³) | $\tau \times 10^5$ Km |
|---|---|---|---|---|---|---|---|---|---|---|---|
| A1 | 0.062 | 0.938 | 81 | 19884.56 | 56.17 | 6.76 | 28.8 | 55.66 | 0.401 | 141.98 | 1.39 |
| A2 | 0.098 | 0.902 | 79 | 20096.24 | 57.09 | 6.87 | 29.4 | 56.80 | 0.414 | 145.60 | 1.37 |
| A3 | 0.145 | 0.855 | 78 | 20372.60 | 58.04 | 6.98 | 30.2 | 58.33 | 0.429 | 150.49 | 1.36 |
| E | 0.18 | 0.82 | 76 | 20578.40 | 58.96 | 7.09 | 30.8 | 59.50 | 0.442 | 154.26 | 1.35 |
| A4 | 0.237 | 0.763 | 88 | 20913.56 | 57.93 | 6.97 | 31.8 | 61.46 | 0.445 | 160.63 | 1.38 |
| A5 | 0.348 | 0.652 | 90 | 21566.24 | 59.41 | 7.15 | 33.9 | 65.49 | 0.479 | 174.00 | 1.37 |
| A6 | 0.454 | 0.546 | 96 | 22189.52 | 60.13 | 7.23 | 36.0 | 69.64 | 0.510 | 188.08 | 1.37 |
| A7 | 0.555 | 0.445 | 99 | 22783.40 | 61.25 | 7.37 | 38.3 | 73.89 | 0.545 | 202.90 | 1.35 |
| A8 | 0.604 | 0.396 | 100 | 23071.52 | 61.85 | 7.44 | 39.4 | 76.08 | 0.565 | 210.64 | 1.35 |
| A9 | 0.651 | 0.349 | 111 | 23347.88 | 60.8 | 7.31 | 40.5 | 78.26 | 0.569 | 218.44 | 1.38 |
| A10 | 0.744 | 0.256 | 120 | 23894.72 | 60.8 | 7.31 | 42.9 | 82.82 | 0.598 | 235.07 | 1.38 |
| A11 | 0.833 | 0.167 | 122 | 24418.04 | 61.82 | 7.44 | 45.3 | 87.53 | 0.640 | 252.67 | 1.37 |
| A12 | 0.918 | 0.082 | 127 | 24917.84 | 62.29 | 7.49 | 47.8 | 92.40 | 0.678 | 271.28 | 1.36 |
| NA | 1 | 0 | 128 | 25400.00 | 63.34 | 7.62 | 50.5 | 97.48 | 0.726 | 291.17 | 1.34 |
| VA | 0 | 1 | 84 | 19520.00 | 54.68 | 6.58 | 27.8 | 53.75 | 0.381 | 135.99 | 1.41 |

**Mixing functions**

Integral molar free energy of mixing ($\Delta G^M$), molar entropy of mixing ($\Delta S^M$) and molar enthalpy of mixing ($\Delta H^M$) and partial thermodynamic mixing functions of the binary alloys when two components are mixed together were determined by using the following equations

$\Delta G^M = RT\ (\chi_{NA}\ \text{lnaNA} + \chi VA\ \text{lnaVA})$ (2)

$\Delta S^M = -R\ (\chi NA\ \ln\chi NA + \chi VA\ \ln\chi VA)$ (3)

$\Delta H^M = RT\ (\chi NA\ \ln\chi NA + \chi VA\ \ln\chi VA)$ (4)

G-iM = μ-iM = RT lnali (5)

Where G-iM (μ-iM) is the partial molar free energy of mixing of component i (mixing chemical potential)in binary mix and ⍰i and ai is the activity coefficient and activity of component respectively. The negative value[18,19] of integral molar free energy of mixing for E and $A_1$ – $A_9$ alloys (Table 2) suggests that the mixing in all cases is spontaneous. The positive value of $\Delta G^M$ for $A_{10}$ – $A_{12}$ suggests there is non-spontaneous mixing in these non eutectic alloys. The integral molar enthalpy of mixing value corresponds to the value of excess integral molar free energy of the system favors the regularity in the binary solutions.

**Table 2: Value of partial and integral mixing of Gibbs free energy($\Delta G^M$), enthalpy($\Delta H^M$) and entropy($\Delta S^M$) of NA-VA system**

| Alloy | $\Delta G_{NA}^{-M}$ J/mol | $\Delta G_{VA}^{-M}$ J/mol | $\Delta G^M$ J/mol | $\Delta H_{NA}^{-M}$ J/mol | $\Delta H_{VA}^{-M}$ J/mol | $\Delta H^M$ J/mol | $\Delta S_{NA}^{-M}$ J/mol/K | $\Delta S_{VA}^{-M}$ J/mol/K | $\Delta S^M$ J/mol/K |
|---|---|---|---|---|---|---|---|---|---|
| A1 | -2977.06 | -164.03 | -338.44 | 5206.74 | 24.34 | -345.65 | 23.12 | 0.532 | 1.93 |
| A2 | -3103.74 | -273.39 | -550.76 | 3693.96 | 28.46 | -387.68 | 19.31 | 0.858 | 2.67 |
| A3 | -3167.08 | -328.07 | -739.72 | 2468.05 | 129.08 | -468.23 | 16.06 | 1.302 | 3.44 |
| E | -3293.77 | -437.42 | -951.56 | 1681.87 | 138.40 | -416.22 | 14.26 | 1.65 | 3.92 |
| A4 | -2533.67 | 218.71 | -433.60 | 1787.37 | 1030.60 | -1209.93 | 11.97 | 2.249 | 4.55 |
| A5 | -2406.98 | 328.07 | -623.73 | 778.66 | 1618.90 | -1326.49 | 8.78 | 3.556 | 5.37 |
| A6 | -2026.93 | 656.13 | -561.98 | 395.63 | 2512.60 | -1551.50 | 6.56 | 5.031 | 5.73 |
| A7 | -1836.91 | 820.17 | -654.51 | -15.90 | 3324.40 | -1470.51 | 4.90 | 6.732 | 5.71 |
| A8 | -1773.57 | 874.85 | -724.80 | -210.04 | 3747.50 | -1357.16 | 4.19 | 7.702 | 5.58 |
| A9 | -1076.81 | 1476.30 | -185.77 | 293.59 | 4837.10 | -1879.27 | 3.57 | 8.752 | 5.38 |
| A10 | -506.733 | 1968.40 | 126.90 | 459.48 | 6420.50 | -1985.50 | 2.46 | 11.33 | 4.73 |
| A11 | -380.05 | 2077.76 | 30.40 | 220.01 | 7955.40 | -1511.82 | 1.52 | 14.88 | 3.75 |
| A12 | -63.3416 | 2351.15 | 134.65 | 221.19 | 10669.0 | -1077.88 | 0.71 | 20.79 | 2.36 |

**Activity and activity coefficient**

The values of activity and activity coefficient of components in the alloys of the system under investigation have been calculated from the equation[20] given below

$$-ln\chi_i^1\gamma_i^1 = \frac{\Delta H_i}{R}\left(\frac{1}{T_e}-\frac{1}{T_i}\right) \quad (6)$$

Where $\gamma_i^1$ and $\chi_i^1$ are activity coefficient and mole fraction of the component *i* in the liquid phase respectively. ΔHi is the heat of fusion of component i at melting point $T_i$ and R is the gas constant. Te is the melting temperature of alloy. Using the values of activity and activity coefficient of the components in alloys mixing and excess thermodynamics functions have been computed.

**Excess thermodynamic functions**

In order to unfold the nature of the interactions between the components forming the eutectic, non-eutectic alloys and addition compound, the excess thermodynamic functions such as integral excess integral free energy ($g^E$), excess integral entropy ($s^E$) and excess integral enthalpy ($h^E$) were calculated using the following equations

$$g^E = RT(\chi_{NA}\ln\gamma_{NA} + \chi_{VA}\ln\gamma_{VA}) \quad (7)$$

$$s^E = -R\left((\chi_{NA}\ln\gamma_{NA} + \chi_{VA}\ln\gamma_{VA} + \chi_{NA}T\frac{\delta\ln\gamma_{NA}}{\delta T} + \chi_{VA}T\frac{\delta\ln\gamma_{VA}}{\delta T}\right) \quad (8)$$

$$h^E = -RT^2\left(\chi_{NA}\frac{\delta\ln\gamma_{NA}}{\delta T} + \chi_{VA}\frac{\delta\ln\gamma_{VA}}{\delta T}\right) \quad (9)$$

and excess chemical potential or excess partial free energy of mixing

$$g_i^{-E} = \mu_i^{-M} = RT\ln\gamma_i^1 \quad (10)$$

The values of $\delta\ln\gamma_i^1/\delta T$ can be determined by the slope of liquidus curve near the alloys form in the phase diagram. The values of the excess thermodynamic functions are given in Table 3. The value of the excess free energy is a measure of the departure of the system from ideal behavior. The reported excess thermodynamic data substantiate the earlier conclusion of an appreciable interaction between the parent components during the formation of alloys. The positive value[21,22] of integral excess free energy for all the eutectic and non-eutectic alloys indicates the possibility of a weaker association between unlike molecules and of stronger interactive nature between like molecules. The excess entropy is a measure of the change in configurational energy due to a change in potential energy and indicates an increase in randomness.

**Gibbs-Duhem equation**

Further the partial molar quantity, activity and activity coefficient can also be determined by using Gibbs-Duhem equation[23,24]

$$\sum\chi_i dz_i^{-M} = 0 \quad (11)$$

$$or\ \ \chi_{NA}dH_{NA}^{-M} + \chi_{VA}dH_{VA}^{-M} = 0 \quad (12)$$

$$or\ \ dH_{NA}^{-M} = \frac{\chi_{VA}}{\chi_{NA}}dH_{VA}^{-M} \quad (13)$$

$$or\ \ [H_{NA}^{-M}]_{\chi_{NA}=y} = \int_{\chi_{NA}=y}^{\chi_{NA}=1}\frac{\chi_{VA}}{\chi_{NA}}dH_{VA}^{-M} \quad (14)$$

Using equation (14) a graph (Fig. 2) between $H_{VA}^{-M}$ and $\chi_{VA}/\chi_{NA}$ gives the solution of the partial molar heat of mixing of a constituent NA in binary alloy and plot between $\chi_{VA}/\chi_{NA}$ vs $\ln\chi_{VA}$ determines the value of activity coefficient (Fig. 3) of component NA in binary alloys.

**Table 3: Value of partial and integral excess Gibbs free energy($g^E$), enthalpy($h^E$) and entropy($s^E$) of NA-VA system**

| Alloy | $g_{NA}^{-E}$ J/mol | $g_{VA}^{-E}$ J/mol | $g^E$ J/mol | $h_{NA}^{-E}$ J/mol | $h_{VA}^{-E}$ J/mol | $h^E$ J/mol | $s_{NA}^{-E}$ J/mol/K | $s_{VA}^{-E}$ J/mol/K | $s^E$ J/mol/K |
|---|---|---|---|---|---|---|---|---|---|
| A1 | 5206.744 | 24.3441 | 345.653 | 310689.43 | 2694.87 | 21790.53 | 862.95 | 7.5438 | 60.579 |
| A2 | 3693.963 | 28.455 | 387.675 | 289948.32 | 14741.79 | 41712.03 | 813.22 | 41.799 | 117.4 |
| A3 | 2468.052 | 129.082 | 468.233 | 151202.26 | 10430.09 | 30842.06 | 423.74 | 29.348 | 86.535 |
| E | 1681.87 | 138.399 | 416.224 | 87117.06 | 5178.87 | 19927.74 | 244.8 | 14.443 | 55.907 |
| A4 | 1787.369 | 1030.57 | 1209.93 | 29460.19 | -2479.55 | 5090.171 | 76.656 | -9.723 | 10.749 |
| A5 | 778.6568 | 1618.89 | 1326.49 | 100522.7 | 47690.27 | 66075.96 | 274.78 | 126.92 | 178.37 |
| A6 | 395.6325 | 2512.61 | 1551.5 | 24469.72 | 21946.76 | 23092.18 | 65.241 | 52.667 | 58.376 |
| A7 | -15.9021 | 3324.36 | 1470.51 | 36790.52 | 58043.45 | 46248.07 | 98.942 | 147.09 | 120.37 |
| A8 | -210.039 | 3747.54 | 1357.16 | -2418.84 | 15532.08 | 4689.724 | -5.922 | 31.594 | 8.9345 |
| A9 | 293.5913 | 4837.07 | 1879.27 | -15984.11 | -1956.26 | -11088.4 | -42.39 | -17.69 | -33.77 |
| A10 | 459.4841 | 6420.49 | 1985.5 | 9118.52 | 80799.45 | 27468.84 | 22.033 | 189.26 | 64.843 |
| A11 | 220.0135 | 7955.39 | 1511.82 | 21317.59 | 213508.5 | 53413.47 | 53.412 | 520.39 | 131.4 |
| A12 | 221.1897 | 10668.6 | 1077.88 | 18071.90 | 467153.2 | 54896.56 | 44.627 | 1141.2 | 134.55 |

**Stability Function**

Thermodynamic behavior of the present system in form of stability and excess stability functions[24,25] can be determined by the second derivative of their molar free energy and excess energy respectively with respect to the mole fraction of either constituent:

$$Stability = \frac{\partial^2 \Delta G^M}{\partial \chi^2} = -2RT \frac{\partial \ln a}{\partial (1-\chi)^2} \quad (15)$$

$$Excess\ Stability = \frac{\partial^2 g^E}{\partial \chi^2} = -2RT \frac{\partial \ln \gamma}{\partial (1-\chi)^2} \quad (16)$$

These values were calculated by multiplying the slope of lna vs $(1-\chi)^2$ and lnγ vs $(1-\chi)^2$ plots with -2RT. The best polynomial equation of the curve generated is given as:

$$\ln\gamma = 3.68(1-\chi)^2 - 21.44(1-\chi)^4 + 81.99(1-\chi)^6 - 146.84(1-\chi)^8 + 126(1-\chi)^{10} - 41.47(1-\chi)^{12} \quad (17)$$

The slope of the curve shown in figure as obtained by differentiating the above equation with respect to $(1-\chi)^2$ may also be used to calculate the excess stability of the NA-VA system. The values of total stability to the ideal stability and defined as

$$Ideal\ Stability = \frac{RT}{\chi(1-\chi)} \quad (18)$$

These values show there is considerable thermodynamic stability in the alloy. The fig. 4 for the stability, excess stability and ideal stability in the form of composition and partial Gibb's energy favors the formation of the binary alloys and their mixing.

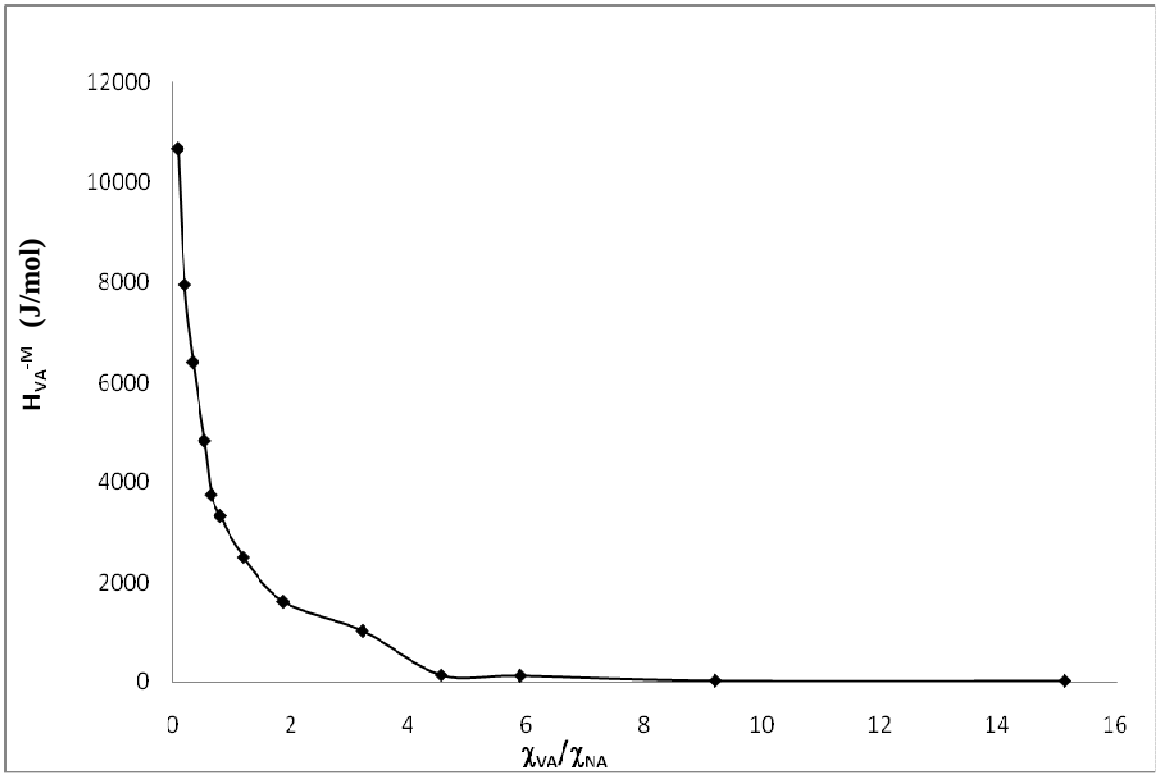


**Fig. 2: Graph between $\chi_{VA}/\chi_{NA}$ vs $H_{VA}^{-M}$**

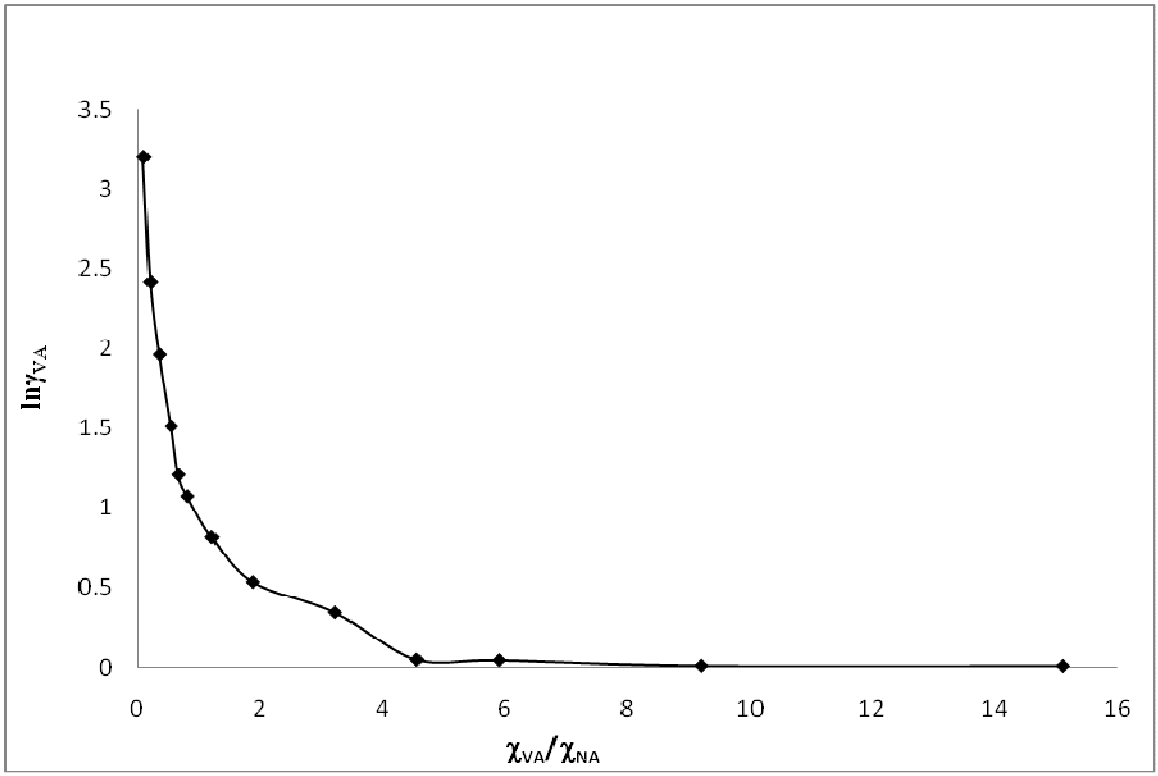


**Fig. 3: Graph between lng$_{VA}$ vs $\chi_{VA}/\chi_{NA}$**

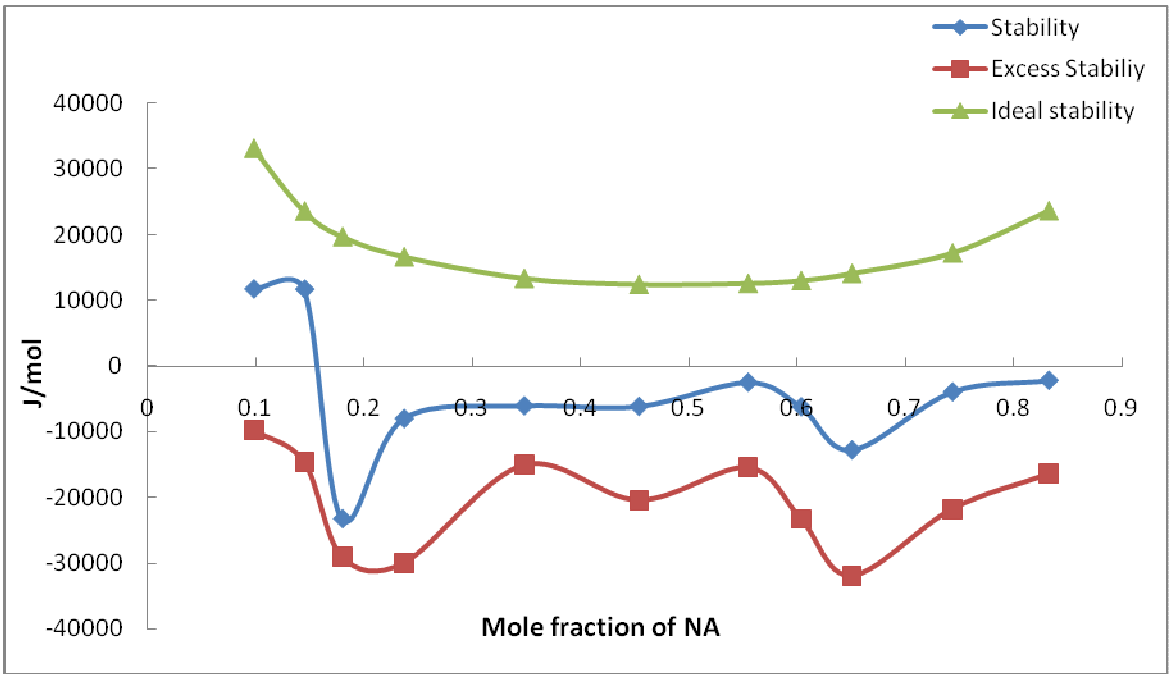


**Fig. 4: Stability Graph of NA-VA**

**INTERFACIAL STUDIES**

**The effective entropy change ($\Delta S_v$)**

It is obvious that the effective entropy change and the volume fraction of phases in the alloy are inter-related to decide the interface morphology during solidification and the volume fraction of the two phases depends on the ratio of effective entropy change of the phases. The entropy of fusion value of alloys is calculated by heat of fusion values of the materials. The effective entropy change per unit volume ($\Delta S_V$) is given by:

$$\Delta S_V = \frac{\Delta H}{T} \cdot \frac{1}{V_m} \quad (19)$$

where $\Delta H$ is the enthalpy change, $T$ is the melting temperature and $V_m$ is the molar volume of solid phase. The entropy of fusion per unit

volume ($\Delta S_V$) for NA and VA was found 0.726 and 0.381 $JK^{-1}cm^{-3}$ respectively. Values of $\Delta S_V$ for alloys are reported in Table 1.

**The solid-liquid interfacial energy (σ)**

It has been found that an experimentally observed value of interfacial energy 'σ' keeps a variation of 50-100% from one worker to other. However, Akbulut and Marasli[26] were calculated the solid-liquid interfacial energy ($\sigma$) from melting enthalpy change and values obtained are found in good agreement with the experimental values. Turnbull empirical relationship between the interfacial energy and enthalpy change provides the clue to determine the interfacial energy value of alloy and is expressed as:

$$\sigma = \frac{C\Delta H}{(N)^{1/3}(V_m)^{2/3}} \quad (20)$$

where the coefficient $C$ lies between 0.33 to 0.35 for nonmetallic system, $V_m$ is molar volume and $N$ is the Avogadro's constant. The value of the solid-liquid interfacial energy of nicotinamide and vanillin was found to be 50.46 and 27.82 $kJm^{-2}$ respectively and σ value of alloys was given in Table 1.

**The driving force of nucleation ($\Delta G_v$)**

The theories of solidification process in past have been discussed on the basis of diffusion model, kinetic characteristics of nucleation and on thermodynamic features. The lateral motion of rudimentary steps in liquid phase advances stepwise with non-uniform surface at low driving force while continuous and uniform surface advances at sufficiently high driving force. The driving force of nucleation/volume free energy during solidification ($\Delta G_V$) is determined by using the following equation

$\Delta G_V = \Delta S_v \Delta T$ (21)

It is opposed by the increase in surface free energy due to creation of a new solid-liquid interface. By assuming that solid phase nucleates as small spherical cluster of radius arising due to random motion of atoms within liquid. The value of $\Delta G_V$ *is* shown it the table 4.

**Table 4: Value of volume free energy change ($\Delta G_v$) during solidification for NA - VA system of different undercoolings (ΔT)**

| Alloy | $\Delta G_v$ ($J/cm^3$) | | | | | |
|---|---|---|---|---|---|---|
| | **1.0** | **1.5** | **2.0** | **2.5** | **3.0** | **3.5** |
| A1 | 0.401 | 0.602 | 0.802 | 1.003 | 1.203 | 1.404 |
| A2 | 0.414 | 0.62 | 0.827 | 1.034 | 1.241 | 1.448 |
| A3 | 0.429 | 0.643 | 0.858 | 1.072 | 1.286 | 1.501 |
| E | 0.442 | 0.663 | 0.884 | 1.105 | 1.326 | 1.547 |
| A4 | 0.445 | 0.667 | 0.89 | 1.112 | 1.335 | 1.557 |
| A5 | 0.479 | 0.719 | 0.959 | 1.198 | 1.438 | 1.678 |
| A6 | 0.51 | 0.765 | 1.019 | 1.274 | 1.529 | 1.784 |
| A7 | 0.545 | 0.818 | 1.091 | 1.364 | 1.636 | 1.909 |
| A8 | 0.565 | 0.847 | 1.129 | 1.412 | 1.694 | 1.977 |
| A9 | 0.569 | 0.853 | 1.138 | 1.422 | 1.707 | 1.991 |
| A10 | 0.598 | 0.897 | 1.196 | 1.495 | 1.794 | 2.094 |
| A11 | 0.64 | 0.96 | 1.279 | 1.599 | 1.919 | 2.239 |
| A12 | 0.678 | 1.017 | 1.356 | 1.696 | 2.035 | 2.374 |
| NA | 0.726 | 1.089 | 1.452 | 1.815 | 2.178 | 2.541 |
| VA | 0.381 | 0.571 | 0.762 | 0.952 | 1.143 | 1.333 |

**The critical radius(r*)**

During liquid-solid transformation embryos are rapidly dispersed in unsaturated liquid and on undercooling liquid becomes saturated and provide embryo of a critical size with radius r* for nucleation which can be expressed by the Chadwick relation[27]:

$$r^* = \frac{2\sigma}{\Delta G_V} = \frac{2\sigma T}{\Delta H_V \Delta T} \quad (22)$$

where σ is the interfacial energy and $\Delta T$ and $\Delta H_V$ are the melting temperature and the enthalpy of fusion of the compound per unit volume, respectively. The critical size of the nucleus for the components and alloys was calculated at different undercoolings and values are found in the range of 39 – 146 nm (Table 5). It can be inferred from table that the size of the critical nucleus decreases with increase in the undercooling of the melt. The existence of embryo and a range of embryo size can be expected in the liquid in any temperature.

**Table 5: Critical size of nucleus (r*) at different undercoolings (ΔT)**

| Alloy | r*(nm) | | | | | |
|---|---|---|---|---|---|---|
| | **1.0** | **1.5** | **2.0** | **2.5** | **3.0** | **3.5** |
| A1 | 143.67 | 95.780 | 71.835 | 57.468 | 47.890 | 41.049 |
| A2 | 142.17 | 94.778 | 71.083 | 56.866 | 47.389 | 40.619 |
| A3 | 140.85 | 93.900 | 70.425 | 56.340 | 46.950 | 40.243 |
| E | 139.37 | 92.910 | 69.683 | 55.746 | 46.455 | 39.819 |
| A4 | 142.99 | 95.328 | 71.496 | 57.197 | 47.664 | 40.855 |
| A5 | 141.45 | 94.297 | 70.723 | 56.578 | 47.148 | 40.413 |
| A6 | 141.44 | 94.292 | 70.719 | 56.575 | 47.146 | 40.411 |
| A7 | 140.26 | 93.506 | 70.129 | 56.103 | 46.753 | 40.074 |
| A8 | 139.47 | 92.983 | 69.737 | 55.790 | 46.491 | 39.850 |
| A9 | 142.42 | 94.948 | 71.211 | 56.969 | 47.474 | 40.692 |
| A10 | 143.34 | 95.559 | 71.670 | 57.336 | 47.780 | 40.954 |
| A11 | 141.66 | 94.441 | 70.831 | 56.665 | 47.220 | 40.475 |
| A12 | 141.05 | 94.031 | 70.523 | 56.419 | 47.016 | 40.299 |
| NA | 138.99 | 92.660 | 69.495 | 55.596 | 46.330 | 39.711 |
| VA | 146.08 | 97.388 | 73.041 | 58.433 | 48.694 | 41.738 |

**Critical free energy of nucleation (ΔG*)**

To form critical nucleus, it requires an activation/localized critical free energy of nucleation (ΔG*) which is evaluated as:

$$\Delta G^* = \frac{16}{3}\frac{\pi\sigma^3}{\Delta G_v^2} \quad (23)$$

The value of ΔG* has been found in the range of $10^{-15}$ to $10^{-16}$ J at different undercoolings, and has been reported in Table 6.

**Gibbs-Thomson coefficient ($\tau$)**

For a planar grain boundary on planar solid-liquid interface the Gibbs-Thomson coefficient ($\tau$) for the system can be calculated by the Gibbs-Thomson Equation is expressed as

$$\tau = r\Delta T = \frac{TV_m\sigma}{\Delta H} = \frac{\sigma}{\Delta S_V} \quad (24)$$

where τ is the Gibbs-Thomson coefficient, $\Delta T$ is the dispersion in equilibrium temperature and, r is the radius of grooves of interface. The theoretical basis of determination of τ was made for equal thermal conductivities of solid and liquid phases for some transparent materials. It was also determined by the help of Gunduz and Hunt[28] numerical method for materials having known grain boundary shape, temperature gradient in solid and the ratio of thermal conductivity of the equilibrated liquid phases to solid phase ($R = K_L/K_S$).The Gibbs-Thomson coefficient for NA, VA and their alloys are found in the range of 1.342 - 1.411 x $10^{-05}$ Km and is reported in Table 1.

**Interfacial Grain boundary energy ($\sigma_{gb}$)**

Grain boundary is the internal surface which can be understood in a very similar way to nucleation on surfaces in liquid-solid transformation. In past, a numerical method is applied to observe the interfacial grain boundary energy ($\sigma_{gb}$) without applying the temperature gradient for the grain boundary groove shape. For isotropic interface there is no difference in the value of interfacial tension and interfacial energy. A considerable force is employed at the grain boundary groove in anisotropic interface. The grain boundary energy can be obtained by the equation:

$$\sigma_{gb} = 2\sigma\cos\theta \quad (25)$$

where θ is equilibrium contact angle precipitates at solid-liquid interface of grain boundary. The grain boundary energy could be twice the solid-liquid interfacial energy in the case where the contact angle tends to zero. The value of $\sigma_{gb}$ for solid NA and VA was found to be 97.48 and 53.75 $kJm^{-2}$ respectively and the value for all alloys is given in Table 1.

**Interface morphology**

The solid-liquid interface morphology can be predicted from the value of the entropy of fusion. According to Hunt and Jackson[29], the type of growth from a binary melt depends upon a factor α, defined as:

$$\alpha = \xi\frac{\Delta H}{RT} = \xi\frac{\Delta S}{R} \quad (26)$$

where $\xi$ is a crystallographic factor depending upon the geometry of the molecules and has a value less than or equal to one. ΔS/R, also known as Jackson's roughness parameter (α) is dimensionless entropy of fusion and R is the gas constant. When α is less than two the solid-liquid interface is atomically rough and exhibits non-faceted growth. The value of Jackson's roughness parameter (ΔS/R) is given in Table 1. For all the alloys the α value was found greater than 2 which indicate the faceted growth proceeds in all the cases.

**Table 6: Value of critical free energy of nucleation (ΔG*) for alloys of NA - VA system at different undercooling(ΔT)**

| Alloy | $\Delta G^* \times 10^{16}$ (J) | | | | | |
|---|---|---|---|---|---|---|
| | **1.0** | **1.5** | **2.0** | **2.5** | **3.0** | **3.5** |
| A1 | 29.5 | 11.1 | 6.23 | 3.99 | 2.77 | 2.03 |
| A2 | 24.9 | 11.1 | 6.23 | 3.98 | 2.77 | 2.03 |
| A3 | 25.1 | 11.2 | 6.28 | 4.02 | 2.79 | 2.05 |
| E | 25.1 | 11.1 | 6.27 | 4.01 | 2.79 | 2.05 |
| A4 | 27.3 | 12.1 | 6.81 | 4.36 | 3.03 | 2.23 |
| A5 | 28.4 | 12.6 | 7.11 | 4.55 | 3.16 | 2.32 |
| A6 | 30.2 | 13.4 | 7.55 | 4.83 | 3.36 | 2.47 |
| A7 | 31.5 | 14.0 | 7.88 | 5.05 | 3.50 | 2.57 |
| A8 | 32.1 | 14.3 | 8.03 | 5.14 | 3.57 | 2.62 |
| A9 | 34.4 | 15.3 | 8.61 | 5.51 | 3.83 | 2.81 |
| A10 | 36.9 | 16.4 | 9.23 | 5.91 | 4.10 | 3.01 |
| A11 | 38.1 | 16.9 | 9.53 | 6.10 | 4.23 | 3.11 |
| A12 | 39.9 | 17.7 | 9.97 | 6.10 | 4.43 | 3.25 |
| NA | 40.8 | 18.2 | 10.2 | 6.54 | 4.54 | 3.33 |
| VA | 24.9 | 11.1 | 6.22 | 3.98 | 4.76 | 2.03 |

**CONCLUSION**

Due to strong solubilizing effect of Nicotinamide, it is assumed to enhance the drugs solubility and dissociation rate of various therapeutics. The present system NA-VA shows the formation of a eutectic with two incongruent melting addition compounds. The mixing Gibb's free energy of all the alloys suggests there is spontaneous mixing in the system. The positive value of excess free energy for all the eutectic and non-eutectic alloys indicates the possibility of stronger interactive nature between like molecules and a weaker association between like molecules. The negative partial molar Gibb's free energy value (fig. 4) favours the overall thermodynamic stability in all the alloys. The critical radius of all the alloys leads at different undercoolings in nano-scale. The value of Jackson's roughness parameter (α) was found greater than 2 which suggest the faceted growth proceeds in all the cases.

**ACKNOWLEDGEMENT**

Thanks are due to the Head Department of Chemistry, V K S University Ara 802301, India for providing research facilities.

**REFERENCES**

1. Del Sole R, Lazzoi MR, Vasapollo G. Synthesis of nicotinamide-based molecularity microspheres and in vitro controlled release studies. Drug Deliv 2010;17(3):130-137.

2. Bryn SR, Xu W, Newman AW. Chemical reactivity in solid-state pharmaceuticals: formulation implications. Adv Drug Del Rev 2001;48:115-136.
3. Remenar JF et al. Crystal engineering of novel cocrystals of a Triazole Drug with 1,4-Dicarboxylic acids. J Am Chem Soc 2003;125:8456-8457.
4. Rao MRP et al. Binary and ternary solid dispersions of fenofibrate for solubility enhancement. Int J Pharm Pharm Sci 2012;4(4):511-517.
5. Goodman A, Gilman A. The Pharmacological Basis of Therapeutics, 11th ed. McGraw Hill, 2006. p 1635-1638.
6. Haider SM. Syntesis of 7-Azaindole and Nicotinamide Derivatives Having Potential Therapeutic Activity. PhD thesis 1995. University of Karachi, Karachi.
7. Ansari MT et al. Improved physicolchemical characteristics of artemisinin-nicotinamide solid dispersions by solvent evaporation and freeze dried methods. Pak J Pharm Sci. 2012;25(2):447-456.
8. Chen A, Zito S, Nash R. Solubility enhancement of nucleoside and structurally related compounds by complex formation. J Pharm Sci. 2009;22(2):234-246.
9. Knip M, Douek IF, Moore WP. Safety of high-dose nicotinamide: a review. Diabetologia. 2000;43:1337.
10. Abraham D et al. Vanillin, a Potential Agent for the Treatment of Sickle Cell Anemia. Blood. 1991;77(6):1334-1341.
11. Sonali SB, Sandip BB, Amrita NB. Interaction and incompatibilities of pharmaceutical excipients with active pharmaceutical ingredients: a comprehensive review. J Excipients and Food Chem 2010;1(3):3-26.
12. Agrwal T, Gupta P, Das SS, Gupta A, Singh NB. Phase equilibria crystallization and microstructural syudies of Naphthalen-2-ol + 1,3-Dinitrobenzene. J Chem Engg Data 2010;55:4206-4210.
13. Sharama BL, Tandon S, Gupta S. Characteristics of the binary faceted eutectic: benzoic Acid-Salicylic Acid system. Cryst Res Technol 2009;44:258.
14. 14.Reddi RSB, Kumar VSA Satuluri, Rai US, Rai RN. Thermal, physicochemical and microstructural studies of binary organic eutectic systems. J Therm Anal Calorim 2012;107:377-385.
15. Tomoaki H, james LF, Mark WP. Assessment of nicotinamide polymorphs by differential scanning calorimetry. Thermochemica Acta 2001;374:85-92.
16. Sangster J. Phase diagrams and thermodynamic properties of Binary system of Drugs. J Phy Chem Data 1999;28;889-930.
17. Seefeldt K, Miller J, Alvarez-Nunez F, Rodriguez-Hornedo N. Crystallization pathways and kinetics of Carbamazepine-Nicotinamide cocystals from the amorphous state by *In Situ* thermomicroscopy, spectroscopy and calorimetry studies. J Pharm Sci 2007;96(5):1147-1158.
18. Shekhar H, Salim SS. Thermodynamic Characteristics of Succinonitrile-Cinnamic acid system. Nat Journal of Jyoti Res. Acad. 2011;5:13-16.
19. Wisniak J, Tamir A. Mixing and excess thermodynamic properties. Phys Sci Data I Elsivier, new York. 1978 p-21-34.
20. Gupta RK, Singh SK, Singh RA. Some physicochemical studies on organic eutectics. J Crystal Growth 2007;300:415-420.
21. Shekhar H, Pandey KB, Kant V. Thermodynamic Characteristics of 1:2 molecular complex of Phthalic anhydride-Camphene system. J Nat Acd Sci Letter 2010;33:153-160.
22. Dwivedi Y, Kant Shiva, Rai SB, Rai RN. Synthesis, Physicochemical and Optical Characterization of Novel Fluorescing Complex: o-Phenylenediamine-Benzoin. J Fluorescence 2011;21:1255-1263.
23. Shamsuddin M, Singh SB, Nasar A. Thermodynamic investigations of liquid gallium-cadmium alloys. Thermochemica Acta 1998;316:11-19.
24. Shekhar H, Kant V. Thermodynamics of pharmaceutical active Nicotinamide based binary alloys. International Research Journal of Pharmacy 2012;3(5):228-233.
25. Shekhar H, Salim SS. Molecular interactions and stability in binary organic alloys. J Nat Acad Sci Letter 2011;34:117-125.
26. Akbulut S, Ocak Y, Keslioglu K, Marasli N. Determination of Interfacial energies in the aminomethylpropanediol – neopentyl glycol organic alloy. Applied Surface Science 2009;255:3594.
27. Chadwick GA. Metallography of Phase Transformation. Butterworths. London. 1972 p.61.
28. Gunduz M, Hunt JD. Acta Metall 1989;37:1839.
29. Hunt JD, Jackson KA. Trans Metall Soc AIME. 1966;236:843.